Pramana – J. Phys. (2019) 92:93
https://doi.org/10.1007/s12043-019-1754-y

Effects of slip on Cu–water or Fe_3O_4–water nanofluid flow over an exponentially stretched sheet

SUDIPTA GHOSH and SWATI MUKHOPADHYAY*

Department of Mathematics, The University of Burdwan, Burdwan 713 104, India
*Corresponding author. E-mail: swati_bumath@yahoo.co.in

MS received 23 December 2017; revised 22 August 2018; accepted 22 November 2018; published online 8 April 2019

Abstract. This study aims to report the boundary layer flow of nanofluid over an exponentially stretched sheet in the presence of velocity slip as well as thermal slip. Utilising similarity transformations, the governing momentum and temperature equations are converted into ordinary differential equations and then solved numerically by shooting technique. An interesting behaviour of the solution for the converted self-similar equations is noted: dual solutions are obtained for some particular range of values of the governing parameters for the flow past an extended sheet. A comparison is made between the boundary layer flow of Cu–water and Fe_3O_4–water nanofluids. Both fluid velocity and temperature increase due to the enhancement in the velocity slip parameter. With the rising values of solid volume fraction, velocity diminishes but temperature increases.

Keywords. Nanofluid; boundary layer flow; exponentially stretching sheet; velocity slip; thermal slip.

PACS Nos **47.15.C; 44.20.+b**

1. Introduction

In recent years, fluid flow due to stretched sheet is a very exciting topic due to its various applications in industries. The problem of boundary layer flow and heat transfer over a linear stretched sheet was considered by a number of researchers. In reality, linearly stretched sheet may not occur always. For this, heat and mass transfer effects for the boundary layer flow of viscoelastic fluid over an exponentially stretched sheet were described by Sanjayanand and Khan [1]. Pal [2] measured the mixed convection flow and heat transfer over an exponentially stretched surface in the presence of a magnetic field. Heat and mass transfer effects for the flow past a stretched surface have been investigated in detail by several researchers which can be found in [3–10].

Nanotechnology has attracted the attention of researchers owing to its extensive applications in areas of manufacturing and medical sciences [11]. The concept of nanofluid has been proposed for increasing the activities of heat-carrying liquids. It was Choi [12] who first realised that the addition of nanoparticles to the base fluid extraordinarily increases the effective thermal conductivity of the fluid. Convective transport in nanofluids was first observed by Buongiorno [13]. He observed that the increase in thermal conductivity occurs due to two main effects: Brownian diffusion and thermophoretic diffusion of nanoparticles. Tiwari and Das [14] proposed a new type of model which became popular. Hydromagnetic flow and heat transfer to a stretched vertical sheet was investigated by Ishak *et al* [15]. The stagnation-point flow of a nanofluid towards a stretched sheet was discussed by Mustafa *et al* [16]. Boundary layer flow of the nanofluid over an exponentially extended surface was studied by Nadeem and Lee [17]. Many research on different aspects of nanofluids can be found in [18–27].

Majority of researchers considered their study with no-slip boundary condition. The no-slip boundary condition is not appropriate in circumstances where surface is adequately silky. Partial slip velocity generally occurs on the elongated boundary for some particular type of fluid such as emulsions, suspensions, foams and polymer solutions. Using homotopy analysis method (HAM), Hayat *et al* [28] obtained analytic solution and reported the effects of slip on a second-grade fluid flow past a stretched sheet embedded in a porous medium. Mukhopadhyay *et al* [29] investigated the heat transfer behaviour of the steady boundary layer flow over a porous moving plate. Sajid *et al* [30] reported the possessions of slip on non-Newtonian Maxwell fluid flow over a stretched sheet. Nanoparticles, being very small in size, are capable to bear slip velocity along with the

molecules of the base fluid [11]. Yet, much attention has not been paid on slip flow of the nanofluid.

To the best of the authors' information, modelling nanofluid flow using Tiwari and Das [14] model due to an exponentially stretched sheet in the presence of slips at the boundary has not yet been addressed. With this motivation, an attempt is made in this paper. Moreover, in this work, a comparative study is carried out between Cu–water and Fe_3O_4–water to realise the nanofluid behaviour clearly. Both velocity and thermal slip conditions at the boundary are taken into account. Self-similar equations are obtained by applying similarity transformations. Numerical solutions of the problem under consideration are then acquired. Basically, in this case, self-similar equations are numerically evaluated. Comparisons are made with the available results in the open literature and complete agreements are found with those results. It is found that the solid volume fraction and slip parameters significantly influence the flow and thermal fields.

2. Mathematical formulation of the problem

Consider the steady two-dimensional boundary layer flow of water-based nanofluids over an exponentially stretched sheet with partial slip boundary conditions. By considering Tiwari and Das [14] model, the governing equations may be written in the usual notation under boundary layer approximations as follows:

$$\frac{\partial u}{\partial x}+\frac{\partial \upsilon}{\partial y}=0, \tag{1}$$

$$u\frac{\partial u}{\partial x}+\upsilon\frac{\partial u}{\partial y}=\nu_{\mathrm{nf}}\frac{\partial^2 u}{\partial y^2}, \tag{2}$$

$$u\frac{\partial T}{\partial x}+\upsilon\frac{\partial T}{\partial y}=\frac{\kappa_{\mathrm{nf}}}{\left(\rho c_p\right)_{\mathrm{nf}}}\frac{\partial^2 T}{\partial y^2}. \tag{3}$$

The velocity components in x and y directions are denoted by u and υ, respectively. $\nu_{\mathrm{nf}}=\mu_{\mathrm{nf}}/\rho_{\mathrm{nf}}$ denotes the kinematic viscosity of the nanofluid where μ_{nf} is the viscosity of the nanofluid and ρ_{nf} is the density of the nanofluid, T denotes the temperature, the thermal conductivity of the nanofluid is represented by κ_{nf} and the specific heat capacitance of the nanofluid is $(\rho c_p)_{\mathrm{nf}}$. The effective fluid properties are given by [31]

$$\rho_{\mathrm{nf}}=(1-\phi)\rho_{\mathrm{f}}+\phi\rho_s,$$

$$\frac{\kappa_{\mathrm{nf}}}{\kappa_{\mathrm{f}}}=\frac{(2\kappa_{\mathrm{f}}+\kappa_{\mathrm{s}})-2\phi\,(\kappa_{\mathrm{f}}-\kappa_{\mathrm{s}})}{(2\kappa_{\mathrm{f}}+\kappa_{\mathrm{s}})+\phi\,(\kappa_{\mathrm{f}}-\kappa_{\mathrm{s}})},$$

$$\mu_{\mathrm{nf}}=\frac{\mu}{(1-\phi)^{2.5}},\ \left(\rho c_p\right)_{\mathrm{nf}}=(1-\phi)\left(\rho c_p\right)_{\mathrm{f}}+\phi\left(\rho c_p\right)_{\mathrm{s}}.$$

The boundary conditions can be expressed as follows:

$$u=U_w+B'\upsilon_{\mathrm{f}}\frac{\partial u}{\partial y},\quad \upsilon=0\ \text{ at } y=0$$

$$\text{and } u\to 0 \text{ as } y\to\infty, \tag{4a}$$

$$T=T_w+D'\frac{\partial T}{\partial y}\ \text{at } y=0 \text{ and } T\to T_\infty$$

$$\text{as } y\to\infty, \tag{4b}$$

where $U_w=c\exp(x/L)$ is the velocity of extension where $c>0$ is constant.

$T_w=T_\infty+T_0\exp(x/2L)$ is the variable temperature at the sheet with T_0 being a constant which measures the rate of temperature increase along the sheet. Here $B'=B_1\mathrm{e}^{-(x/2L)}$ and $D'=D_1\mathrm{e}^{-(x/2L)}$ are, respectively, the velocity slip and thermal slip factors.

2.1 *Similarity transformations*

Let us now introduce the stream function ψ as $u=\partial\psi/\partial y$ and $\upsilon=-\partial\psi/\partial x$ and consider the following similarity transformations:

$$\psi=\sqrt{2\nu_{\mathrm{f}}Lc}f(\eta)\exp\left(\frac{x}{2L}\right),\quad \theta(\eta)=\frac{T-T_\infty}{T_w-T_\infty},$$

$$\eta=y\sqrt{\frac{c}{2\nu_{\mathrm{f}}L}}\exp\left(\frac{x}{2L}\right), \tag{5}$$

where η is the similarity variable.

Equation (1) is automatically satisfied. Using relation (5) in eqs (2) and (3), we obtain the following equations:

$$\frac{1}{(1-\phi)^{2.5}\left(1-\phi+\phi(\rho_{\mathrm{s}}/\rho_{\mathrm{f}})\right)}f'''+ff''-2f'^2=0, \tag{6}$$

$$\frac{\kappa_{\mathrm{nf}}/\kappa_{\mathrm{f}}}{1-\phi+\phi\left(\left(\rho c_p\right)_{\mathrm{s}}/\left(\rho c_p\right)_{\mathrm{f}}\right)}\theta''+\mathrm{Pr}\left(f\theta'-f'\theta\right)=0, \tag{7}$$

where $\mathrm{Pr}=(\mu c_p)_{\mathrm{f}}/\kappa_{\mathrm{f}}$ is the Prandtl number.

The boundary conditions take the following forms:

$$f(\eta)=0,\ f'(\eta)=1+Bf''(\eta)\ \text{ at } \eta=0,$$

$$f'(\eta)\to 0 \text{ as } \eta\to\infty, \tag{8}$$

$$\theta(\eta)=1+D\theta'(\eta)\ \text{ at } \eta=0,$$

$$\theta(\eta)\to 0 \text{ as } \eta\to\infty. \tag{9}$$

$B=B_1\sqrt{c\nu_{\mathrm{f}}/2L}$ and $D=D_1\sqrt{c/2\nu_{\mathrm{f}}L}$ are, respectively, the velocity slip and thermal slip parameters.

The local skin friction coefficient and Nusselt number for this problem are given by

$$C_{\mathrm{f}} = \frac{\mu_{\mathrm{nf}}}{\rho_{\mathrm{f}} U_w^2 \mathrm{e}^{2x/L}} \left.\frac{\partial u}{\partial y}\right|_{y=0},$$

$$\mathrm{Nu}_x = -\frac{x\kappa_{\mathrm{nf}}}{\kappa_{\mathrm{f}}(T_w - T_\infty)} \left.\frac{\partial T}{\partial y}\right|_{y=0}, \tag{10}$$

$$Cf_x \mathrm{Re}_x^{1/2} = \frac{1}{(1-\phi)^{2.5}} f''(0),$$

$$\mathrm{NuRe}_x^{-1/2} = -\left(\frac{\kappa_{\mathrm{nf}}}{\kappa_{\mathrm{f}}}\right)\theta'(0). \tag{11}$$

3. Numerical method for solution

Equations (6) and (7) are nonlinear ordinary differential equations. These equations subject to the boundary conditions (8) and (9) form a boundary value problem which is solved numerically by converting it to an initial value problem using Runge–Kutta method with a combination of shooting technique. Choosing the step length 0.01, setting the convergence criteria as 10^{-6}, numerical computation was carried out. A suitable finite value of η_∞ is required. Here, $\eta_\infty = 15$ is chosen so that the far-field boundary conditions given by the last part of eqs (8) and (9) are satisfied, i.e. $f'(15) \to 0,\ \theta(15) \to 0$.

4. Results and discussions

4.1 *Verification of the results*

The precision of the numerical method measured for this problem is tested by direct comparisons with available values of $f''(0)$ reported by Magyari and Keller [32], Elbashbeshy [33] and Sahoo and Poncet [34] in the absence of nanoparticle volume fraction and velocity slip parameter. The value of velocity gradient at the wall, obtained as $f''(0) = -1.281812$, correct to six decimal places, agrees perfectly with $f''(0) = -1.28180$ [32], $f''(0) = 1.28181$ [33] and $f''(0) = -1.281811$ [34] which motivates us to carry out our computations for

Table 1. Thermophysical properties of water, Fe_3O_4 [36] and Cu [35].

	$\rho\,(\mathrm{kg/m^3})$	$C_p\,(\mathrm{J/kg\,K})$	$\kappa\,(\mathrm{W/m\,K})$
Water	997.1	4179	0.613
Fe_3O_4	5180	670	9.7
Cu	8933	385	400

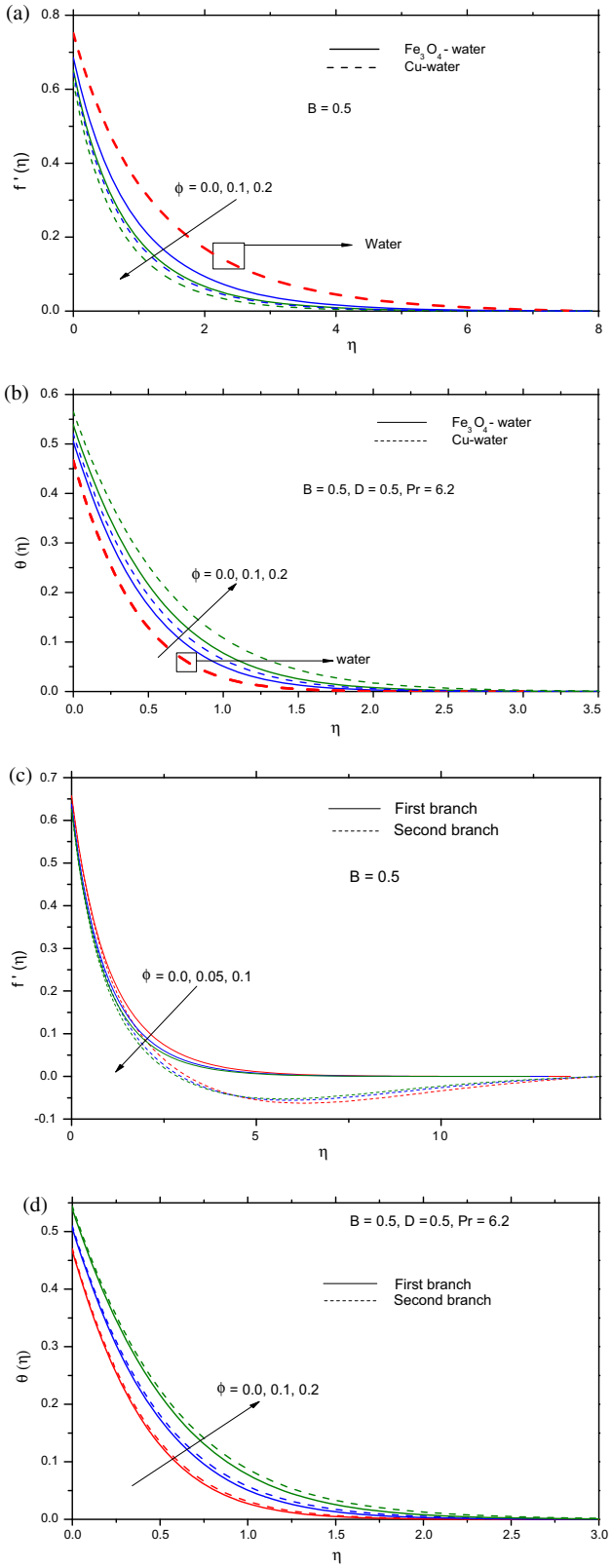

Figure 1. Effect of nanoparticle volume fraction ϕ on (**a**) velocity $f'(\eta)$ and (**b**) temperature $\theta(\eta)$. Dual (**c**) velocity and (**d**) temperature profiles for the variation of nanoparticle volume fraction ϕ.

other parametric values for the complete understanding of the flow and heat transfer behaviours.

4.2 *Analysis of the results*

To investigate the flow behaviours of Cu–water and Fe_3O_4–water, numerical computations are made with different parametric values, whereas the thermophysical values of Cu–water [35] and Fe_3O_4–water [36] are provided in table 1.

Interesting behaviour of fluid flow is noted for this particular problem. Dual solutions exist for some particular values of the leading parameters. Generally, dual solutions exist for flow past a shrinking sheet. Here, dual solutions exist for stretching sheet problem.

The effects of nanoparticle volume fraction on velocity and temperature profiles are shown in figures 1a and 1b. It can be observed that fluid velocity diminishes but temperature increases due to the increase of nanoparticle volume fraction ϕ. Here, $\phi = 0$ stands for pure water (in the absence of nanoparticles). Fluid velocity is highest for pure water (i.e. in the absence of nanoparticles). It can be observed that the velocity of Fe_3O_4–water is greater than that of Cu–water. Due to the presence of nanoparticles, the thermal conductivity of the fluid is enhanced. With the rise in nanoparticle volume fraction ϕ, shear stress also increases, and as a result, fluid velocity decreases. Moreover, large thermal conductivity goes together with the large thermal diffusivity. A drop in the temperature gradients is occurred due to the high value of thermal diffusivity, and consequently, the boundary layer thickness increases as can be seen in figure 1b. It is also noticed that the thermal boundary layer thickness of Cu–water is greater than that of Fe_3O_4–water. In the absence of nanoparticles, lowest temperature is noted for water (figure 1b).

The dual velocity and temperature profiles for the variations of nanoparticle volume fraction ϕ for Fe_3O_4–water are shown in figures 1c and 1d, respectively. Same type of effect is noted here. Among the two branches of solutions, first branch gives the stable solution, whereas the second branch is mathematically important but physically not relevant. Stability analysis can be found easily in the open literature, and so it is excluded here.

Figures 2a and 2b show the effects of velocity slip parameter on velocity and temperature profiles, respectively. Velocity boundary layer thickness

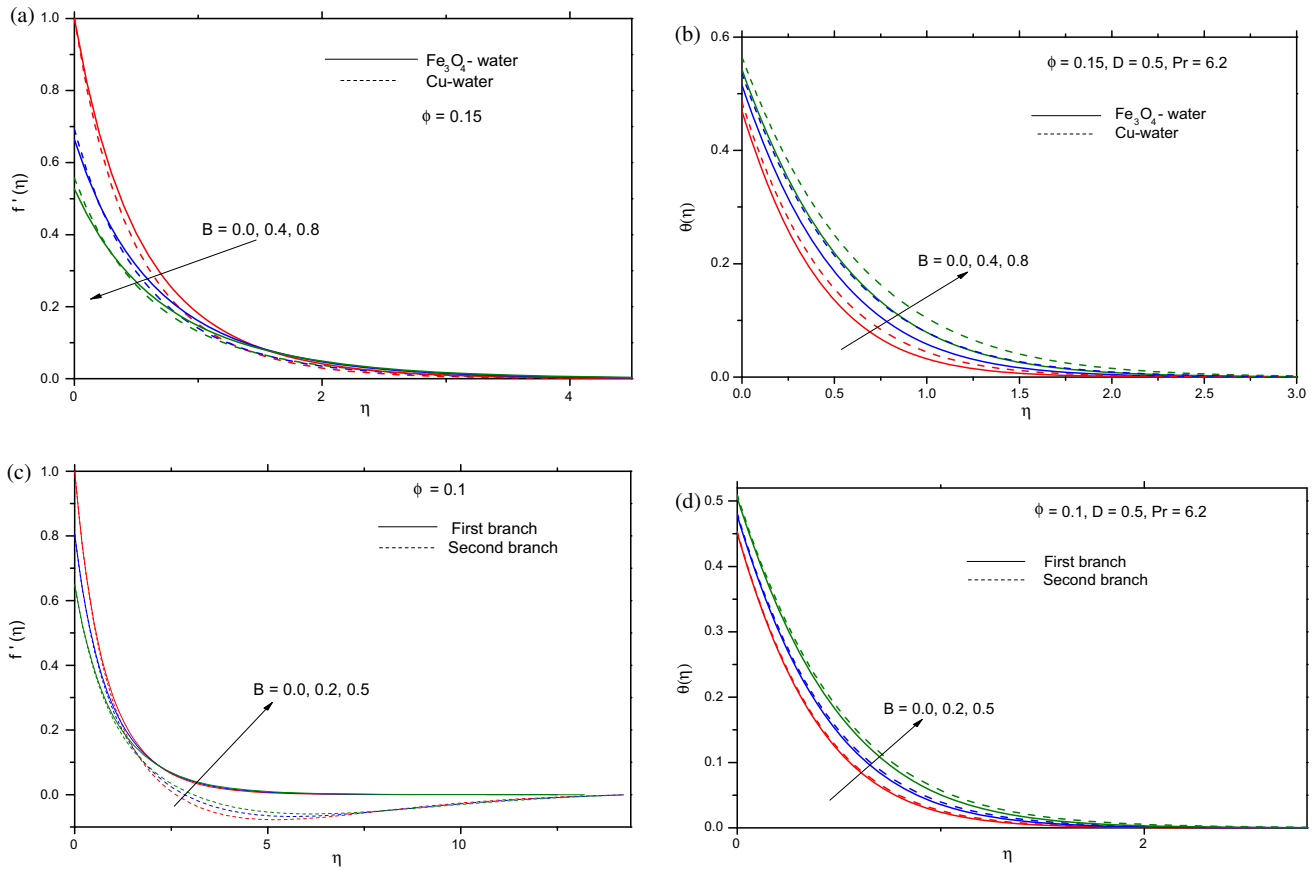

Figure 2. Effect of velocity slip parameter B on (**a**) velocity $f'(\eta)$ and (**b**) temperature $\theta(\eta)$. Dual (**c**) velocity and (**d**) temperature profiles for the variation of slip parameter B.

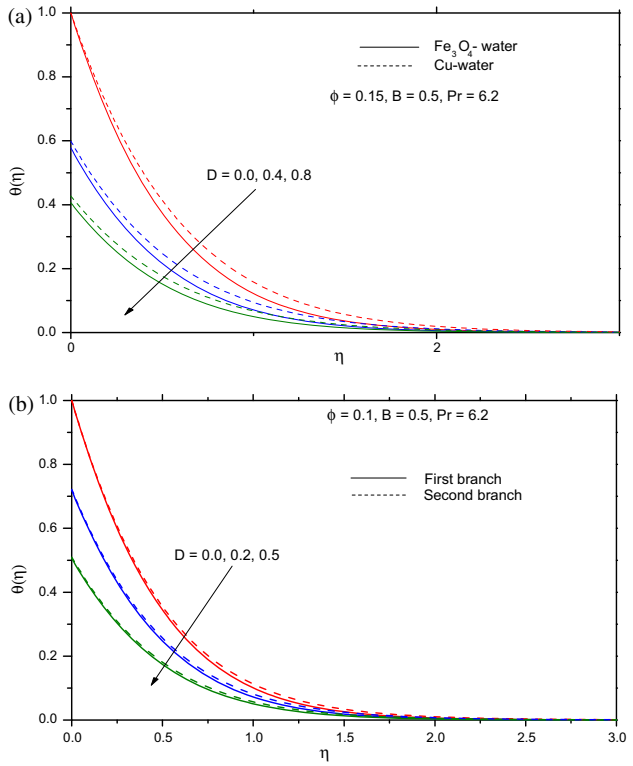

Figure 3. Effect of thermal slip parameter D on (**a**) temperature $\theta(\eta)$ and (**b**) dual temperature profiles.

decreases (figure 2a) and temperature boundary layer thickness increases (figure 2b) with the rise in velocity slip parameter B. It can be observed that the flow velocity initially drops off but increases away from the sheet. Due to slip, the velocity of fluid nearer to the sheet is no longer equal to the velocity of extension of the sheet. With the rising values of the slip parameter B, slip velocity increases. As a result, fluid velocity reduces since the pulling of the extending sheet being capable of partly transmission to the fluid under the slip condition at the boundary. Fluid velocity is higher for Fe_3O_4–water than for Cu–water (figure 2a). Temperature rises appreciably with the increasing values of velocity slip parameter B (figure 2b). Temperature of Cu–water is higher than that of Fe_3O_4–water (figure 2b). Here also, the dual nature of velocity and temperature is noted.

The dual velocity and temperature profiles for the variations of velocity slip parameter B for Fe_3O_4–water are presented in figures 2c and 2d, respectively.

The thermal boundary layer thickness reduces due to the enhancement of thermal slip parameter which is shown in figures 3a and 3b. With the rise in thermal slip parameter D, less heat is transported to the fluid. As a result, the temperature of the fluid reduces (figures 3a and 3b). In figure 3a, the temperature of Cu–water is

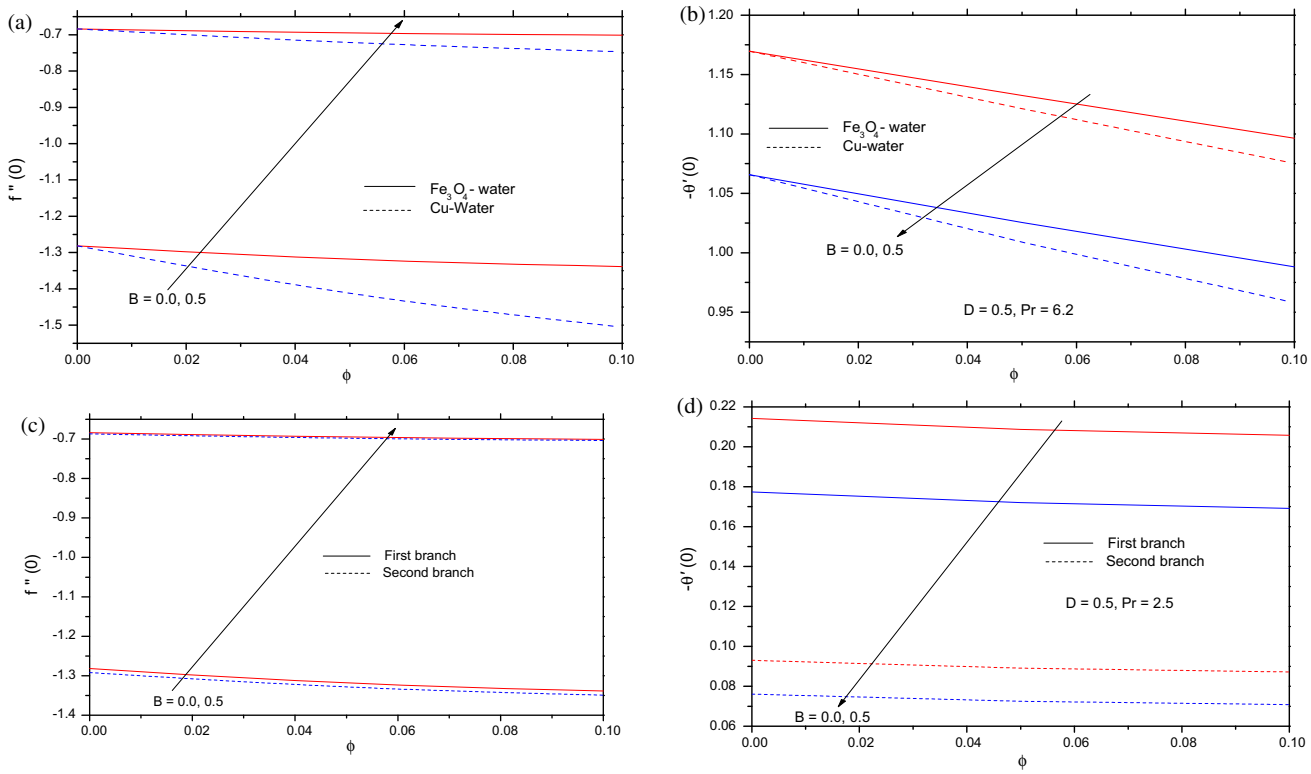

Figure 4. Variations of (**a**) $f''(0)$, (**b**) $[-\theta'(0)]$, (**c**) dual branches of $f''(0)$ and (**d**) dual branches of $[-\theta'(0)]$ with velocity slip parameter B for different values of nanoparticle volume fraction ϕ.

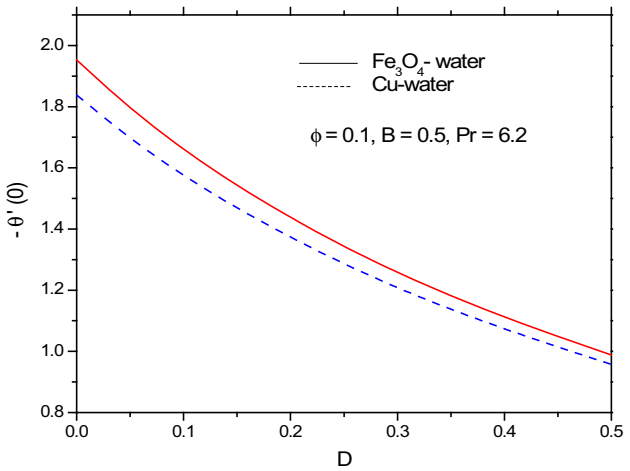

Figure 5. Variations of $[-\theta'(0)]$ with thermal slip parameter D.

higher than that of Fe_3O_4–water. The dual temperature profiles can be viewed in figure 3b.

The effects of velocity slip parameter and nanoparticle volume fraction on local skin friction coefficient and local Nusselt number are shown in figures 4a–4d. Wall shear stress increases with the rise in nanoparticle volume fraction ϕ. Local skin friction coefficient increases due to the increase in velocity slip parameter B but decreases with the increase in nanoparticle volume fraction ϕ (figures 4a and 4c). Skin friction is higher for Fe_3O_4–water than for Cu–water (figure 4a). From figures 4b and 4d, it is noted that local Nusselt number decreases with the increase in both nanoparticle volume fraction ϕ and velocity slip parameter B. Nusselt number is higher for Fe_3O_4–water than for Cu–water (figure 4b). Physically, the nanoparticles drive away energy in the form of heat energy. Simultaneous accumulation of much more nanoparticles may put forth more energy which augments the temperature. Basically, the heat flux is enhanced by the accumulation of nanoparticles, i.e. with the rise in nanoparticle volume fraction ϕ. Consequently, the thermal boundary layer becomes thicker. Figures 4c and 4d show the dual nature of wall shear stress and heat transfer coefficient. Figure 5 shows that the local Nusselt number drops off with the enlarged values of thermal slip parameter D as less amount of heat is transported to the fluid from the sheet.

Streamlines are shown in figures 6a and 6b for Cu–water and Fe_3O_4–water, respectively. Streamlines for Cu–water (figure 6a) are more dense than those for Fe_3O_4–water (figure 6b).

5. Concluding remarks

Boundary layer steady flow of nanofluid over an exponentially elongated sheet in the presence of velocity slip as well as thermal slip has been examined considering Tiwari and Das model for Cu–water and Fe_3O_4–water nanofluids. From the observations, the following remarks can be made:

(i) Dual solutions are obtained for the problem.
(ii) The presence of nanoparticles helps to slow down the motion of nanofluids.
(iii) The velocity boundary layer thickness reduces due to the enhancement in the nanoparticle volume fraction.
(iv) Rate of transfer of heat energy at the surface can be enhanced by the addition of nanoparticles.
(v) The thermal boundary layer thickness enhances due to increase in the nanoparticle volume fraction.

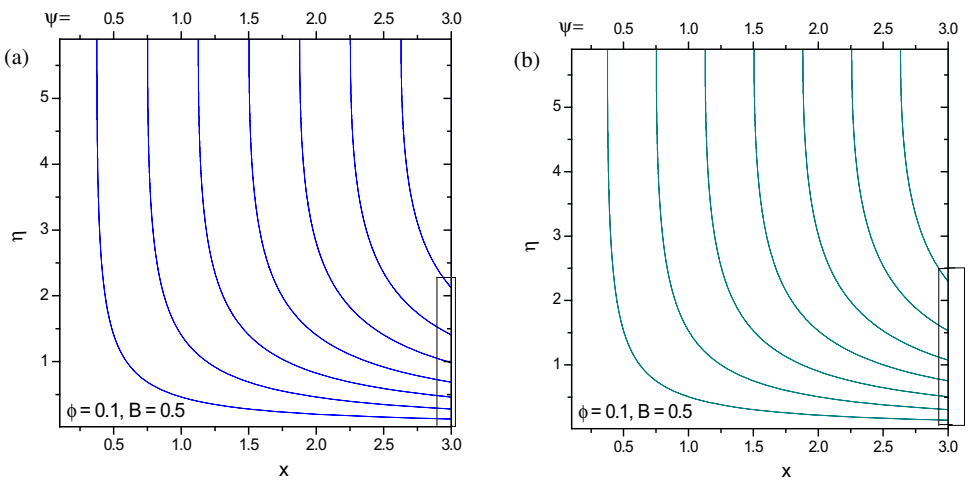

Figure 6. Streamlines for (**a**) Cu–water and (**b**) Fe_3O_4–water.

(vi) Flow becomes slower with the rise in the velocity slip.
(vii) Transfer of heat from the sheet to the fluid slows down with the rise in thermal slip.

Acknowledgements

Thanks are indeed due to the reviewers for their constructive suggestions which helped a lot in improving the quality of this paper. S Mukhopadhyay acknowledges financial support received from SERB, New Delhi, India, through Young Scientist Project (YSS/2014/000681).

References

[1] E Sanjayanand and S K Khan, *Int. J. Therm. Sci.* **45**, 819 (2006)
[2] D Pal, *Appl. Math. Comput.* **217**(**6**), 2356 (2010)
[3] T Hayat, M Sajid and I Pop, *Nonlinear Anal.: Real World Appl.* **9**, 1811 (2008)
[4] T Hayat, M Qasim and Z Abbas, *Z. Natforsch. A* **65**, 231 (2010)
[5] T Hayat, M Mustafa and S Asghar, *Nonlinear Anal.: Real World Appl.* **11**, 3186 (2010)
[6] T Hayat, Z Iqbal, M Qasim and S Obaidat, *Int. J. Heat Mass Transf.* **55**, 1817 (2012)
[7] T Hayat, M Imtiaz, A Alsaedi and S Almezal, *J. Magn. Magn. Mater.* **401**, 296 (2016)
[8] M Khan, L Ahmad and M Ayaz, *Pramana – J. Phys.* **91**: 13 (2018)
[9] M Khan, M Irfan, W A Khan and M Ayaz, *Pramana – J. Phys.* **91**: 14 (2018)
[10] Z Iqbal, Z Mehmood and B Ahmad, *Pramana – J. Phys.* **90**: 64 (2018)
[11] S T Hussain, S Nadeem and R Ul Haq, *Eur. Phys. J. Plus* **129**, 161 (2014)
[12] S U S Choi, In: *The Proceedings of the ASME International Mechanical Engineering Congress and Exposition* (San Francisco, USA, 1995) Vol. 66, p. 99
[13] J Buongiorno, *J. Heat Transf.* **128**, 240 (2006)
[14] R K Tiwari and M K Das, *Int. J. Heat Mass Transf.* **50**, 2002 (2007)
[15] A Ishak, R Nazar and I Pop, *Heat Mass Transf.* **44**, 921 (2008)
[16] M Mustafa, T Hayat, I Pop, S Asghar and S Obaidat, *Int. J. Heat Mass Transf.* **54**, 5588 (2011)
[17] S Nadeem and C Lee, *Nanoscale Resc. Lett.* **7**(**94**), 1 (2012)
[18] T Hayat, T Abbas, M Ayub, M Farooq and A Alsaedi, *J. Mol. Liq.* **222**, 854 (2016)
[19] A Mushtaq, M Mustafa, T Hayat and A Alsaedi, *Adv. Powder Technol.* **27**, 2223 (2016)
[20] T Hayat, M Waqas, S A Shehzad and A Alsaedi, *Pramana – J. Phys.* **86**(**1**), 3 (2016)
[21] A A Afify and Md Abd El-Aziz, *Pramana – J. Phys.* **88**: 31 (2017)
[22] A Alsaedi, M I Khan, M Farooq, N Gull and T Hayat, *Adv. Powder Technol.* **28**, 288 (2017)
[23] M Mustafa, J A Khan, T Hayat and A Alsaedi, *Int. J. Heat Mass Transf.* **108**, 1340 (2017)
[24] M Sheikholeslami, T Hayat and A Alsaedi, *Int. J. Heat Mass Transf.* **108**, 1870 (2017)
[25] T Hayat, N Aslam, A Alsaedi and M Rafiq, *Int. J. Heat Mass Transf.* **115**, 1033 (2017)
[26] T Hayat, S Ahmad, M I Khan and A Alsaedi, *Physica B* **537**, 116 (2018)
[27] M Sheikholeslami, T Hayat and A Alsaedi, *J. Mol. Liq.* **249**, 941 (2018)
[28] T Hayat, T Javed and Z Abbas, *Int. J. Heat Mass Transf.* **51**, 4528 (2008)
[29] S Mukhopadhyay, K Bhattacharyya and G C Layek, *Int. J. Heat Mass Transf.* **54**(**13–14**), 2751 (2011)
[30] M Sajid, Z Abbas, N Ali, T Javed and I Ahmad, *Walailak J. Sci. Tech.* **11**, 1093 (2014)
[31] B Mahanthesh, B J Gireesha and R S R Gorla, *J. Nigerian Math. Soc.* **35**, 178 (2016)
[32] E Magyari and B Keller, *J. Phys. D* **32**(**5**), 577 (1999)
[33] E M A Elbashbeshy, *Arch. Mech.* **53**(**6**), 643 (2001)
[34] B Sahoo and S Poncet, *Int. J. Heat Mass Transf.* **54**, 5010 (2011)
[35] Nadeem, R Ul Haq and Z H Khan, *Alexandria Eng. J.* **53**, 219 (2014)
[36] M Sheikholeslami and D D Ganji, *Energy* **75**, 400 (2014)